Conference on Modelling Fluid Flow (CMFF'22)
The 18th International Conference on Fluid Flow Technologies
Budapest, Hungary, August 30-September 2, 2022

Identification of data-driven aerodynamic models for reduced-order aeroelastic simulations

János LELKES[1], Dávid András HORVÁTH[2], Tamás KALMÁR-NAGY[3]

[1] Corresponding Author. Department of Fluid Mechanics, Faculty of Mechanical Engineering, Budapest University of Technology and Economics. Bertalan Lajos u. 4 - 6, H-1111 Budapest, Hungary. Tel.: +36 1 463 2464, Fax: +36 1 463 3464, E-mail: lelkes.janos@gpk.bme.hu
[2] Department of Fluid Mechanics, Faculty of Mechanical Engineering, Budapest University of Technology and Economics. E-mail: david_horvath67@yahoo.com
[3] Department of Fluid Mechanics, Faculty of Mechanical Engineering, Budapest University of Technology and Economics. E-mail: kalmar.nagy.tamas@gpk.bme.hu

ABSTRACT

Multiple approaches exist for calculating the time-dependent aerodynamic loads of thin, flexible structures subjected to airflow. For calculating the aerodynamic loads, analytical, semi-empirical, CFD-based, and various reduced-order models exist. These models are usually only applicable for small deformations; in the case of large deformations, calculating aerodynamic loads is computationally costly. In this paper, a data-based identification method to calculate the aerodynamic loads was applied. The most significant advantage of this technique is that it is also accurate for large structure deformations. After the initial data fitting process, the simulations run very quickly. To create the data-based model, we used high-precision validated CFD simulations. The SINDy (Sparse Identification of Nonlinear Dynamics) algorithm was utilized for the model construction. Multiple optimization routines were used to fit the aerodynamic model, e.g., LASSO (Least Absolute Shrinkage and Selection Operator) and STLSQ (Sequentially Thresholded Least Squares). As the result of the paper, we get a data-based aerodynamic model for a single configuration and a compact process, with which the aerodynamic loading of arbitrary moving structures can be calculated in the time domain.

Keywords: Aerodynamics, Aeroelasticity, Nonlinear dynamics, Sparse identification

NOMENCLATURE

NRMS	[1]	normed root mean square error
C_L	[1]	lift coefficient
H_1, A_i	[1]	flutter derivatives
L	[N]	lift force
M	[Nm]	aerodynamic moment
b	[m]	half chord length
c_α	[Ns/rad]	damping of the pitch DoF
c_h	[Ns/m]	damping of the heave DoF
c_i	[SI]	coefficients of the ROM
h	[m]	heave
k	[1]	Reduced frequency
k_α	[N/rad]	stiffness of the pitch DoF
k_h	[N/m]	stiffness of the heave DoF
m	[kg]	mass
q	[1/(s^{2}rad^3)]	stiffness coefficient of the cubic spring
U	[m/s]	wind velocity
α	[rad]	pitch angle
ω	[rad/s]	angular frequency
ω_α	[rad/s]	angular natural frequency of the pitch DoF
ω_h	[rad/s]	angular natural frequency of the heave DoF
ρ	[kg/m^3]	density
ξ_α	[1]	damping factor of the pitch DoF
ξ_h	[1]	damping factor of the heave DoF
I_α	[kgm^2]	moment of inertia

1. INTRODUCTION

Aerodynamic models are essential for designing aircraft, evaluating static and dynamic aeroelastic stability, and developing feedback control laws. Obtaining accurate and efficient aerodynamic models has been a fundamental objective of research efforts in aeronautics over the past century [1]. Closed-form solutions for the attached incompressible unsteady flow problem around a two-dimensional (2D) airfoil exist in both the frequency and time domains [2].

Wagner [3] developed a model for the unsteady lift on a two-dimensional flat plate for arbitrary small-amplitude pitching motion. He computed the effect of idealized planar wake vorticity on the circulation around the plate in response to a step in the angle of attack analytically. After this, the response to arbitrary motion could be constructed by convolution with this indicial response. Ten years later, Theodorsen [4] derived a complementary model to study the aeroelastic problem of flutter instability in the frequency domain. Wagner's and Theodorsen's theories were derived analytically for an idealized two-dimensional flat plate moving through an inviscid, incompressible fluid. The motion of the flat plate is assumed to be infinitesimal, leaving an idealized planar wake.

The finite state flow model offers state equations for the induced flow field itself [5]. The governing equations of the finite state flow model were derived directly from the potential flow equations (either velocity or acceleration potential). Thus, no intermediate steps were invoked in which restrictions were placed on airfoil motions. The theory is an arbitrary-motion theory from the outset. In contrast to Computational Fluid Dynamics (CFD) and vortex lattice methods, the states represent induced flow expansion fields rather than velocities at discrete nodes. As a result, the states are hierarchical, and the equation coefficients are known in closed form. No numerical fitting of frequency-response or indicial functions is needed to apply the finite state flow model.

The dynamic stall phenomenon and its importance for load calculations and aeroelastic simulations are well known. Different models exist to model the effect of the dynamic stall. For dynamic stall, the physics of the flow separation and stall development differs fundamentally from the stall mechanisms observed for the same airfoil under static (quasi-steady) conditions [6].

The effect of dynamic stall can be defined as a delay in the stall onset: stall occurs at a higher angle of attack than for the static stall case. A strong vortex is formed at the leading edge that separates and is convected along the suction surface of the airfoil. This event begins with a rapid increase in lift and ends with complete flow separation and catastrophic loss of lift as the vortex disturbance is convected past the trailing edge of the airfoil. This behavior can produce hysteresis loops in the force coefficients, producing cyclic pressure loads that are not predicted by conventional lift and drag data obtained at steady angles of attack [1].

The ONERA semi-empirical model [7] describes the unsteady airfoil behavior employing a set of nonlinear differential equations. A first-order linear differential equation describes the inviscid (attached flow) aerodynamic contribution, and a second-order differential equation describes the nonlinear viscous effects associated with the stall.

The Beddoes–Leishman method [8] is a dynamic stall model where the emphasis is on a more accurate and complete physical representation of the overall unsteady aerodynamic problem but still in a form that keeps the complexity of analysis down to minimize computational cost. In this way, it attempts to overcome the limitations of other models where many empirically determined coefficients limit the method's applicability. The Beddoes–Leishman model essentially consists of four subsystems: 1. an attached flow model for the unsteady (linear) aerodynamic forces based on Duhamel superposition, 2. a separated flow model for the nonlinear aerodynamic forces, 3. a dynamic stall onset model, 4. a dynamic stall model for the vortex-induced aerodynamic forces.

The nonlinear, second-order dynamic stall model developed by H. Snel [9, 10] is an example of a modern semi-empirical engineering model used to include dynamic stall effects in aeroelastic response codes for wind turbines. This model uses no airfoil-specific parameters in its modeling equations but still can predict the dynamic stall with the same accuracy as models that require such input. This characteristic makes Snel's dynamic stall model desirable for application in an aeroelastic design code where numerous airfoil profiles need to be evaluated, negating the need for any parameter identification from dynamic wind tunnel tests.

Lelkes and Kalmár-Nagy modeled the aerodynamic forces for large angles of attack as a piecewise linear function, which was able to capture the phenomenon of dynamic stall [11].

First, the applied data-driven system identification method is described in this paper. Then, the identified models are presented for three different reduced frequency values compared with the simulation data. Afterward, the models are applied for a simple 2-DOF aeroelastic model of a flat plate.

2. SPARSE IDENTIFICATION OF NONLINEAR DYNAMICAL SYSTEMS

Traditionally, dynamical systems are modeled by first principles, such as Newton's second law. However, this approach can be time-consuming while requiring expert knowledge, and the resulting models can be too simplistic to capture the real-world dynamics accurately. With the advent of powerful computers and efficient machine learning algorithms, modeling based on real-world measurement data becomes possible.

In this paper, we use the Sparse Identification of Nonlinear Dynamical systems (SINDy) method, introduced by Brunton et al. [12, 13], and later refined in the work of Champion et al. [14]. An overview of the method, as well as the description of the Python package that is used in our paper, is given by Silva et al. [15]. Several alternate versions of this method have been proposed. Kaheman et al. [16] introduced SINDy-PI, which is a parallel version that can be used to identify implicit dynamics while being robust to noise. Kaptanoglu et al. [17] proposed a modification of the SINDy algorithm, which is useful for identifying globally stable models. The SINDy method can also be modified to be applicable to various boundary value problems, as shown by Shea et al. [18].

An overview of data-driven methods in aerospace engineering is given by Brunton et al. [19]. In the work of Sun et al. and Pohl et al. [20, 21] the SINDy method is used to derive polynomial models for the lift of an airfoil.

Here, a brief introduction to SINDy is given; more information can be found in the articles mentioned above. Our aim is to determine a model for a dynamical system in the following form:

$$\dot{\underline{x}}(t) = \underline{f}\left(\underline{x}, t\right), \tag{1}$$

where $\underline{x}$ is the vector of the state variables, and t is the time variable. We want to determine the function $\underline{f}$. The idea of the SINDy method is that usually, $\underline{f}$ has a sparse representation in the space of the possible functions. Due to this, a sparse regression is used to discover $\underline{f}$. Let us denote

$$\underline{\underline{X}} = \begin{bmatrix} \underline{x}^T(t_1) \\ \vdots \\ \underline{x}^T(t_n) \end{bmatrix}, \tag{2}$$

$$\dot{\underline{\underline{X}}} = \begin{bmatrix} \dot{\underline{x}}^T(t_1) \\ \vdots \\ \dot{\underline{x}}^T(t_n) \end{bmatrix}, \tag{3}$$

where we measure the state vector $\underline{x}$ at $t_1, \ldots, t_n$ time points, and either also measure the derivative of the state vector, or calculate it numerically from $\underline{x}$. The feature library is denoted by $\underline{\underline{\Theta}}\left(\underline{\underline{X}}\right)$, for example, for a polynomial library

$$\underline{\underline{\Theta}}\left(\underline{\underline{X}}\right) = \left[\underline{\underline{1}} \quad \underline{\underline{X}} \quad \underline{\underline{X}}^{P_2} \cdots\right], \tag{4}$$

where $\underline{\underline{X}}^{P_2}$ denotes the second order polynomials

$$\underline{\underline{X}}^{P_2} = \begin{bmatrix} x_1^2(t_1) & x_1(t_1)x_2(t_1) & \cdots & x_2^2(t_1) & \cdots & x_m^2(t_1) \\ \vdots & \vdots & \ddots & \vdots & \ddots & \vdots \\ x_1^2(t_n) & x_1(t_n)x_2(t_n) & \cdots & x_2^2(t_n) & \cdots & x_m^2(t_n) \end{bmatrix}. \tag{5}$$

We are searching for the vector $\underline{\underline{\Xi}} = \left[\xi_1 \quad \cdots \quad \xi_m\right]$

$$\dot{\underline{\underline{X}}} = \underline{\underline{\Theta}}\left(\underline{\underline{X}}\right)\underline{\underline{\Xi}}. \tag{6}$$

Once this is found, a model can be constructed as follows

$$\dot{\underline{x}} = \underline{f}\left(\underline{x}\right) = \underline{\underline{\Theta}}\left(\underline{x}^T\right)\underline{\underline{\Xi}}. \tag{7}$$

For real-world data, usually $\underline{\underline{X}}$, and $\dot{\underline{\underline{X}}}$ are contaminated with noise, so instead of equation (6) we have

$$\dot{\underline{\underline{X}}} = \underline{\underline{\Theta}}\left(\underline{\underline{X}}\right)\underline{\underline{\Xi}} + \eta \underline{\underline{Z}}, \tag{8}$$

where noise is modeled as a Gaussian distribution with zero mean and η noise magnitude. Numerous objective functions can be used for the sparse regression, we have primarily used the sequentially thresholded least squares (STLSQ), and the least absolute shrinkage and selection operator (LASSO), which are respectively l_2, and l_1 regularized regressions promoting sparsity [12], these will be detailed in the next section.

2.1. SINDy optimizers

The LASSO optimizer is a simple l_1 regularized regression with the following objective function

$$\frac{1}{2n}\left\|\underline{y} - \underline{\underline{X}}\,\underline{w}\right\|_2^2 + \lambda\left\|\underline{w}\right\|_1, \tag{9}$$

where $\underline{y}$ is the training data of the algorithm, $\dot{\underline{\underline{X}}}$ in equation (8), $\underline{\underline{X}}$ is the function library $\underline{\underline{\Theta}}(\underline{\underline{X}})$, $\underline{w}$ is the vector of weights $\underline{\underline{\Xi}}$, and λ is the regularization parameter. The norms are defined the following way

$$\left\|\underline{x}\right\|_1 = \sum_{i=1}^{n}|x_i|, \tag{10}$$

$$\left\|\underline{x}\right\|_2 = \sqrt{\sum_{i=1}^{n}|x_i|^2}, \tag{11}$$

where $\underline{x} = \left[x_1 \quad x_2 \quad \ldots \quad x_n\right]^T$. The other optimizer that we have used is the STLSQ, which was originally proposed to be used with the SINDy algorithm in [12]. It has the following objective function

$$\frac{1}{2n}\left\|\underline{y} - \underline{\underline{X}}\,\underline{w}\right\|_2^2 + \lambda\left\|\underline{w}\right\|_2^2. \tag{12}$$

It can be observed that this is very similar to the objective function that LASSO uses. The only difference is that STLSQ utilizes an l_2 regularization instead of an l_1. However, there is one more important difference. The algorithm works by finding the optimum weights for the objective function and then masking out every coefficient that is lower than a set threshold. Afterward, it iterates these steps for the non-masked-out coefficients. This iteration procedure is useful to promote sparsity in the learned model.

3. IDENTIFIED MODELS

The CFD simulations that the models have been trained on were obtained by prescribing a sinusoidal oscillation for the angle of attack of the flat plate. The details of the CFD simulations are described in [22, 23].

Data were obtained for three oscillation amplitudes and angles of attack, resulting in 9 different time series of the aerodynamic lift force. Three models were identified, one for each frequency. The frequency was nondimensionalized; the resulting reduced frequency is defined as $k = \frac{\omega b}{U}$, where b is the half chord length, U is the wind velocity, and ω is the angular frequency of the oscillation. Reduced frequency is the dimensionless number used in general for the case of unsteady aerodynamics and aeroelasticity [6]. It is one of the parameters that defines the degree of unsteadiness of the problem. The aerodynamic model equations were created by using the

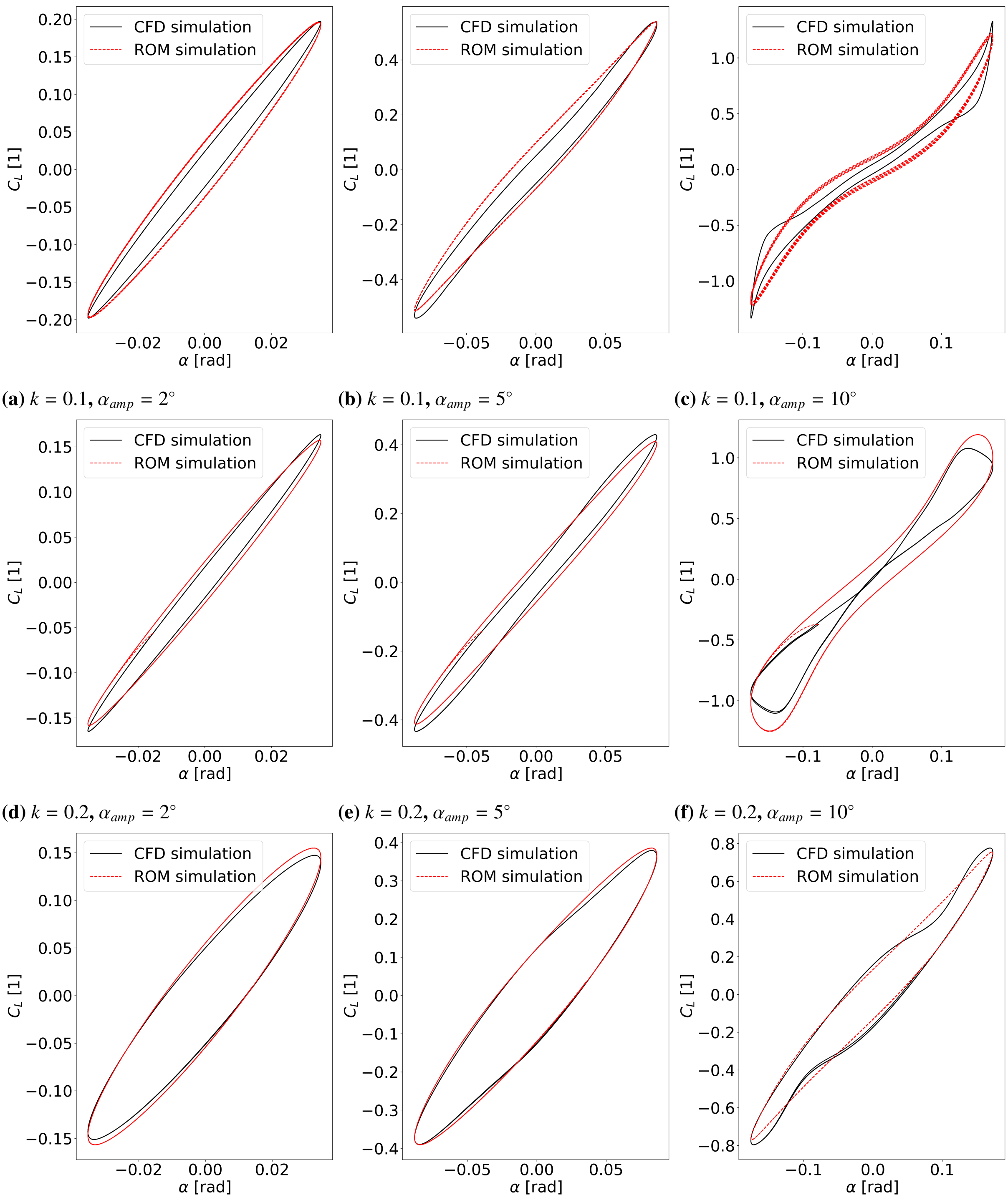

(a) $k = 0.1$, $\alpha_{amp} = 2°$ **(b)** $k = 0.1$, $\alpha_{amp} = 5°$ **(c)** $k = 0.1$, $\alpha_{amp} = 10°$

(d) $k = 0.2$, $\alpha_{amp} = 2°$ **(e)** $k = 0.2$, $\alpha_{amp} = 5°$ **(f)** $k = 0.2$, $\alpha_{amp} = 10°$

(g) $k = 0.5$, $\alpha_{amp} = 2°$ **(h)** $k = 0.5$, $\alpha_{amp} = 5°$ **(i)** $k = 0.5$, $\alpha_{amp} = 10°$

Figure 1. Comparison of the identified ROM with the CFD simulation for $k \in \{0.1, 0.2, 0.5\}$ **and** $\alpha_{amp} \in \{2°, 5°, 10°\}$**.**

Reduced frequency	c_1	c_2	c_3	c_4	c_5	c_6	c_7
$k = 0.1$	0.213	5.42	0	249	0	0	-1.52·10^6
$k = 0.2$	12.2	0	-2.70	0	0	0.799	0
$k = 0.5$	4.01	6.32	-1.34	0	-56.5	0.463	0

Table 1. The coefficients of the reduced-order model Eq. (13)**.**

state variables $\alpha,\ \dot\alpha,\ C_L$, where $\alpha,\ \dot\alpha$ are considered as known inputs, which can be measured. The general form of the Reduced-Order Model (ROM) can be written as

$$\dot C_L(\alpha,\dot\alpha,C_L;k) = \begin{aligned}[t] & c_1(k)\alpha + c_2(k)\dot\alpha + c_3(k)C_L \\ & + c_4(k)\alpha^2 + c_5(k)\alpha\dot\alpha + \ldots, \end{aligned} \tag{13}$$

where a lexicographic ordering was used for the coefficients $c_i(k)$, which are listed in Table 1. The fitting procedure is relatively fast, and it takes only a couple of seconds with given optimization parameters such as λ in equations (9), (12).

For the reduced frequency $k = 0.1,\ k = 0.2,\ k = 0.5$, the lift coefficients from the CFD simulation and the fitted model as the a function of the angle of attack for oscillation amplitudes $\alpha_{amp} \in \{2°, 5°, 10°\}$ are shown in Figure 1. These reduced frequencies were chosen because they cover the region of possible values during flutter. We determined the Normed Root Mean Squared Error (NRMS) of the aerodynamic models using the formula

$$\mathrm{NRMS}_{C_L} = \frac{1}{C_{Lmax} - C_{Lmin}} \sqrt{\frac{\sum_{i=1}^{N}\left(C_L - \hat C_L\right)^2}{N}}, \tag{14}$$

where N is the number of data points, C_L is the CFD simulation data, $\hat C_L$, is the predicted value by the ROM simulation, C_{Lmax} is the maximum, while C_{Lmin} is the minimum value of the CFD simulation data. The NRMS for the three models can be found in Table 2. It can be observed that the models provide an excellent fit and can reproduce the nonlinear behavior associated with the high angle of attack and high-frequency oscillations.

Amplitude	$k = 0.1$	$k = 0.2$	$k = 0.5$
2°	2.53%	1.88%	1.66%
5°	2.45%	2.25%	0.94%
10°	3.44%	4.62%	1.61%

Table 2. The NRMS values of the identified aerodynamic models.

4. TEST CASES

In this section, we apply the identified aerodynamic models to a 2-DOF aeroelastic system. In the model, α describes the pitch (positive clockwise), while h is the plunge displacement (positive downward). The mass is m, the moment of inertia around the pitching axis is I_α, the semichord of the wing is b. The spring, and the damping coefficient for the plunge DOF is k_h, c_h, respectively, while these for the pitch are $k_\alpha(\alpha), c_\alpha$ [24].

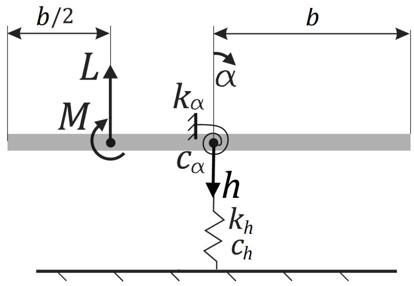

Figure 2. The 2-DOF flat plate

Equations of motion for a simple 2-DOF flat plate (see Figure 2) can be written generally as [25]:

$$m\ddot h + c_h\dot h + k_h h = -L, \tag{15}$$

$$I_\alpha\ddot\alpha + c_\alpha\dot\alpha + k_\alpha(\alpha)\alpha = M, \tag{16}$$

where L and M are the aerodynamic lift and moment, respectively. They can be calculated from the pressure distribution on the surface, i.e.

$$L = \int p d\underline{A}, \tag{17}$$

$$M = \int p x d\underline{A}, \tag{18}$$

where p is the pressure distribution, x is the distance from the point where the lift is applied.

The identified models are now applied to predict flutter for similar parameter values as the training data. We used Eq. (16) in combination with the identified models described in the previous sections to simulate flutter. It needs to be noted that the lift in this model also depends on the plunge state, but when training the SINDy models, we did not take this into account. Due to this, we used Theodorsen's lift theory to model the plunge parts of the lifts.

We have also added a cubic spring to the angular DOF to keep the vibrations inside the applicability region of the model and the better approximate reality in the process, i.e., $k_\alpha(\alpha)\alpha = k_{\alpha 1}\alpha + k_{\alpha 3}\alpha^3$. Using the identified models in Section 3, the lift force and the aerodynamic moment can be expressed as

$$L = \frac{1}{2}\rho U^2 b\left(C_L(k) + \frac{2kH_1(k)}{U}\dot h + \frac{2k^2H_4(k)}{b}h\right) \tag{19}$$

$$M = \frac{1}{2}\rho U^2 b^2 \left(\frac{C_L(k)}{4} + \frac{2kA_1(k)}{U}\dot{h} + \frac{2k^2 A_4(k)}{b}h\right) \quad (20)$$

where $H_1(k), H_4(k), A_1(k), A_4(k)$ are the flutter derivatives of the heave motion [4], and $C_L(k)$ is the identified lift coefficient variable from the pitching motion. Substituting (19) and (20) into (15) and (16) we get

$$\ddot{h} + 2\omega_h\xi_h\dot{h} + \omega_h^2 h = \\ = -\frac{\rho U^2 b}{2m}\left(C_L(k) + \frac{2kH_1(k)}{U}\dot{h} + \frac{2k^2 H_4(k)}{b}h\right), \quad (21)$$

$$\ddot{\alpha} + \omega_\alpha\xi_\alpha\dot{\alpha} + \omega_\alpha^2\alpha + q\alpha^3 = \\ = \frac{\rho U^2 b^2}{2I_\alpha}\left(\frac{C_L(k)}{4} + \frac{2kA_1(k)}{U}\dot{h} + \frac{2k^2 A_2(k)}{b}h\right), \quad (22)$$

where $q = k_{\alpha^3}/I_\alpha$ is the stiffness coefficient of the cubic spring, $\xi_h = \xi_\alpha = \xi$ is the damping factor, and ω_h, ω_α are the angular natural frequencies of the h, and α degrees of freedom. The evolution of the lift coefficient from the pitching motion is

$$\dot{C}_L(k) = c_1(k)\alpha + c_2(k)\dot{\alpha} + c_3(k)C_L \\ +c_4(k)\alpha^2 + c_5(k)\alpha\dot{\alpha} + \ldots, \quad (23)$$

with the coefficients listed in Table 1. We solve the model equations (21-23) numerically using the Mathematica software. For the numerical solution, we used the following initial conditions

$$h(0) = 0.1\,\mathrm{m},\ \alpha(0) = 0\,\mathrm{rad},\ C_L(0) = 0, \\ \dot{h}(0) = 0\,\mathrm{m/s},\ \dot{\alpha}(\mathrm{rad}/s) = 0\,\mathrm{m}. \quad (24)$$

Figure 3 illustrates the results of the ROM simulation (Eqs. (21-23)) using the parameters from Tables 1 and 3, where $\xi_\alpha = \xi_h = \xi$.

Parameter	$k = 0.1$	$k = 0.5$
ω_h [rad/s]	0.628	3.14
ω_α [rad/s]	0.754	3.267
ξ [1]	0.1	0.1
q [1/(s^{2}rad^3)]	40	10
U [m/s]	1	3

Table 3. Parameters of the ROM

The models determined for $k = 0.1$ and $k = 0.5$ are able to reproduce flutter, as shown in Figure 3. In the case of $k = 0.2$, the simulation showed that divergence occurred, not flutter. From Table 1, it can be observed that in this model, the coefficient of $\dot{\alpha}$ is zero, while for the other two models, it is positive. So in the future, it might be useful to use constrained optimization techniques to prescribe a nonzero value of this coefficient to get more useful models. Although only three models have been fitted, it cannot be certain that this technique will result in better models, so more research is necessary in this direction.

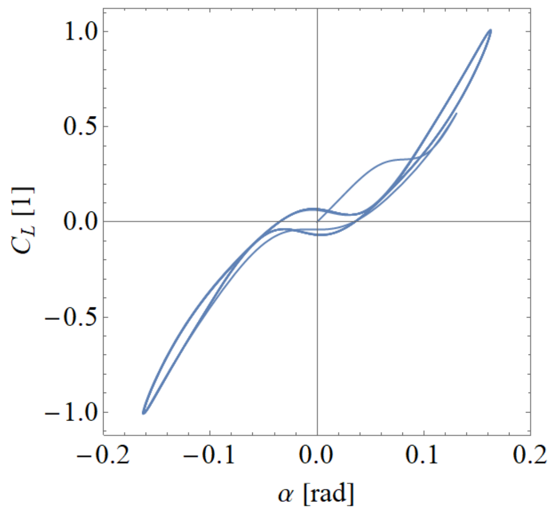

(a) $k = 0.1$

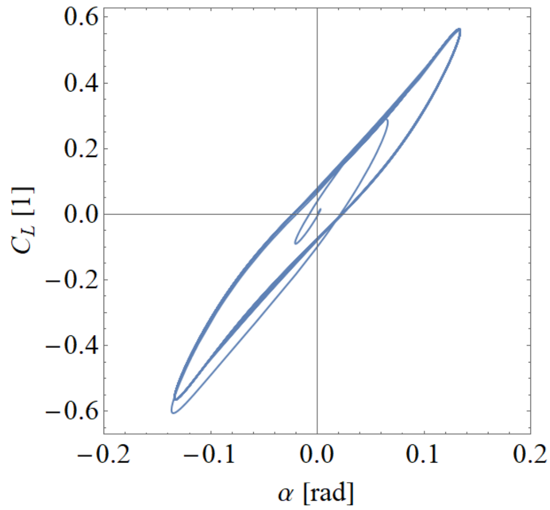

(b) $k = 0.5$

Figure 3. Dynamic lift coefficient for $k = 0.1$, and $k = 0.5$

5. CONCLUSIONS

The significant problem of creating reduced-order models for aerodynamic loads, valid for large amplitude, and frequency oscillations, was studied. The SINDy method was utilized to extract the governing differential equation of the aerodynamic lift coefficient from CFD data of a flat plate with pitching motion. This method resulted in easily interpretable, simple models. It was shown that the identified models for one particular frequency show excellent agreement with the CFD simulation data for varying amplitude oscillations. The test cases showed that some identified models could reproduce the flutter phenomenon. Suggestions to improve the optimization procedure were also given.

ACKNOWLEDGEMENTS

The research reported in this paper and carried out at BME has been supported by the ÚNKP-21-3 New National Excellence Program of the Ministry for Innovation and Technology from the source of the National Research, Development and Innovation Fund, and the NRDI Funds (TKP2020 NC, Grant No. BME-NCS; NKFI K-21 137726) based on the charter of bolster issued by the NRDI Office under the auspices of the Ministry for Innovation and Technology. The research reported in this paper is part of project no. BME-NVA-02, implemented with the support provided by the Ministry of Innovation and Technology of Hungary from the National Research, Development and Innovation Fund, financed under the TKP2021 funding scheme.

REFERENCES

[1] Holierhoek, J., De Vaal, J., Van Zuijlen, A., and Bijl, H., 2013, "Comparing different dynamic stall models", *Wind Energy*, Vol. 16 (1), pp. 139–158.

[2] Boutet, J., and Dimitriadis, G., 2018, "Unsteady lifting line theory using the wagner function for the aerodynamic and aeroelastic modeling of 3d wings", *Aerospace*, Vol. 5 (3), p. 92.

[3] Wagner, H., 1924, "Über die Entstehung des dynamischen Auftriebes von Tragflügeln", .

[4] Theodorsen, T., 1935, "Report No. 496, general theory of aerodynamic instability and the mechanism of flutter", *Journal of the Franklin Institute*, Vol. 219 (6), p. 766–767.

[5] Peters, D. A., Karunamoorthy, S., and Cao, W.-M., 1995, "Finite state induced flow models. I-Two-dimensional thin airfoil", *Journal of Aircraft*, Vol. 32 (2), pp. 313–322.

[6] Leishman, G. J., 2006, *Principles of helicopter aerodynamics with CD extra*, Cambridge University Press.

[7] Tran, C., and Petot, D., 1980, "Semi-empirical model for the dynamic stall of airfoils in view of the application to the calculation of responses of a helicopter blade in forward flight", *ONERA*.

[8] Leishman, J. G., and Beddoes, T., 1989, "A Semi-Empirical model for dynamic stall", *Journal of the American Helicopter society*, Vol. 34 (3), pp. 3–17.

[9] Snel, H., and Schepers, J., "Joint investigation of dynamic inflow effects and implementation of an engineering method", .

[10] Snel, H., 1997, "Heuristic modelling of dynamic stall characteristics", *EWEC-CONFERENCE-*, Bookshop for Scientific Publications, pp. 429–433.

[11] Lelkes, J., and Kalmár-Nagy, T., 2021, "Analysis of a piecewise linear aeroelastic system with and without tuned vibration absorber", *Nonlinear Dynamics*, Vol. 103 (4), pp. 2997–3018.

[12] Brunton, S. L., Proctor, J. L., and Kutz, J. N., 2016, "Discovering governing equations from data by sparse identification of nonlinear dynamical systems", *Proceedings of the National Academy of Sciences*, Vol. 113 (15), p. 3932–3937.

[13] Brunton, S. L., Proctor, J. L., and Kutz, J. N., 2016, "Sparse Identification of Nonlinear Dynamics with Control (SINDYc)", *IFAC-PapersOnLine*, Vol. 49 (18), p. 710–715.

[14] Champion, K., Zheng, P., Aravkin, A. Y., Brunton, S. L., and Kutz, J. N., 2020, "A Unified Sparse Optimization Framework to Learn Parsimonious Physics-Informed Models From Data", *IEEE Access*, Vol. 8, p. 169259–169271.

[15] Silva, B. D., Champion, K., Quade, M., Loiseau, J.-C., Kutz, J., and Brunton, S., 2020, "PySINDy: A Python package for the sparse identification of nonlinear dynamical systems from data", *Journal of Open Source Software*, Vol. 5 (49), p. 2104.

[16] Kaheman, K., Kutz, J. N., and Brunton, S. L., 2020, "SINDy-PI: a robust algorithm for parallel implicit sparse identification of nonlinear dynamics", *Proceedings of the Royal Society A: Mathematical, Physical and Engineering Sciences*, Vol. 476 (2242), p. 20200279.

[17] Kaptanoglu, A. A., Callaham, J. L., Aravkin, A., Hansen, C. J., and Brunton, S. L., 2021, "Promoting global stability in data-driven models of quadratic nonlinear dynamics", *Physical Review Fluids*, Vol. 6 (9).

[18] Shea, D. E., Brunton, S. L., and Kutz, J. N., 2021, "SINDy-BVP: Sparse identification of nonlinear dynamics for boundary value problems", *Physical Review Research*, Vol. 3 (2).

[19] Brunton, S. L., Kutz, J. N., Manohar, K., Aravkin, A. Y., Morgansen, K., Klemisch, J., Goebel, N., Buttrick, J., Poskin, J., Blom-Schieber, A. W., and et al., 2021, "Data-Driven Aerospace Engineering: Reframing the Industry with Machine Learning", *AIAA Journal*, p. 1–26.

[20] Sun, C., Tian, T., Zhu, X., and Du, Z., 2020, "Sparse identification of nonlinear unsteady aerodynamics of the oscillating airfoil", *Proceedings of the Institution of Mechanical Engineers, Part G: Journal of Aerospace Engineering*, Vol. 235 (7), p. 809–824.

[21] Pohl, J., Semaan, R., and Jones, A. R., 2019, "Dynamic lift measurements on an airfoil with periodic flap motion at high Reynolds number", *AIAA Scitech 2019 Forum*.

[22] Lendvai, B., and Lelkes, J., 2021, "Aeroelasztikus szárnymodell numerikus vizsgálata: Numerical analysis of aeroelastic wing model", *Nemzetközi Gépészeti Konferencia–OGÉT*, pp. 48–51.

[23] Lelkes, J., and Lendvai, B., 2021, "Torziós csillapító alkalmazása belebegés megszüntetésére: Application of a torsional absorber for flutter suppression", *Nemzetközi Gépészeti Konferencia–OGÉT*, pp. 44–47.

[24] Lelkes, J., and Kalmár-Nagy, T., 2020, "Analysis of a piecewise linear aeroelastic system with and without tuned vibration absorber", *Nonlinear Dynamics*.

[25] Dowell, E. H., Curtiss, H. C., Scanlan, R. H., and Sisto, F., 1989, *A modern course in aeroelasticity*, Vol. 3, Springer.